Hindawi
Advances in Materials Science and Engineering
Volume 2022, Article ID 4490485, 18 pages
https://doi.org/10.1155/2022/4490485

Research Article

Load Transfer Efficiency Analysis and Void Evaluation of Composite Pavement Cement Concrete Slab

Hao Li,[1,2] **Naren Fang**,[3] **Xuancang Wang**,[1] **Yang Fang**,[2] **Xianghang Li**,[2] **Chao Li**,[2] **and Siyin Ding**[2]

[1]*School of Highway Engineering, Chang'an University, Xi'an 710064, China*
[2]*Foshan Transportation Science and Technology Co.,Ltd., Foshan 528041, Guangdong, China*
[3]*School of Civil Engineering, Tianjin Chengjian University, Tianjin 300384, China*

Correspondence should be addressed to Naren Fang; 2017021044@chd.edu.cn

Received 6 August 2021; Revised 26 January 2022; Accepted 4 March 2022; Published 27 March 2022

Academic Editor: Shengwen Tang

The void at the bottom of a cement concrete slab is a common problem of composite pavements. It is of great significance to evaluate the spring stiffness, void size, and soil base elastic modulus at the bottom of cement concrete slab timely and accurately for the maintenance and guarantee of the pavement performance. In this paper, the composite pavement at a joint is modeled and the load transfer mechanism is realized by using spring groups for simulating the dowels that connect the two slabs of the joint. A database is established based on a large number of simulation results of joint load transfer efficiency and voids and the changing law of load transfer efficiency of cement concrete slab reveals their relationship. Taking into consideration the spring stiffness, void size, and soil base elastic modulus, the void evalua\tion method of composite pavement cement concrete slab is established by using back propagation neural network algorithm. The results show that the void evaluation method can provide the void determination map with two parameters. The values of the two parameters can be determined by the deflection basin. After querying the Atlas, the void determination can be more accurate. The research results provide scientific guidance for the void identification of the composite pavement and can effectively extend the service life of the pavement.

1. Introduction

With the continuous increase of modern traffic, the composite pavement that consists of "asphalt layer + cement concrete slab" (hereinafter referred to as the composite pavement) has been widely implemented. Reflective cracks are the most important "disease" of composite pavements. Experts from all over the world have focused their interest on how to prevent or treat reflective cracks and solve other related pavement problems [1, 2]. Voids of cement concrete slab can be caused by such reflective cracks. These voids can be created due to the existence of reflective cracks, the repeated action of vehicle loads, the rainfall that flows down into the junction of the cement slab and the base layer, which is the weakest point of the pavement structure, and the rainfall that continuously washes the base layer, causing the loss of the support of the cement concrete slab. Therefore, in order to illustrate the phenomenon of void in pavement structure, the authors provide Figures 1–3. Figures 1 and 2 show a schematic diagram of a complete pavement structure without and with voids below the cement concrete slab, respectively, as assumed in this study. The void of the cement concrete slab will cause the loss of the stability of the pavement structure and the performance of the pavement will be significantly reduced [3]. In Figure 3, an actual case of support loss of the cement concrete slab is presented, caused by the sliding of the soil base. Therefore, it is very important to accurately identify the void phenomenon of cement concrete slabs. Generally, "identifying the location and area of voids at the bottom of cement concrete slabs" is collectively referred to as "void evaluation."

Kawamura et al. [4] found out that two indices, namely normalized deflection and peak time difference of deflection, can be used for detecting voids underneath concrete slabs.

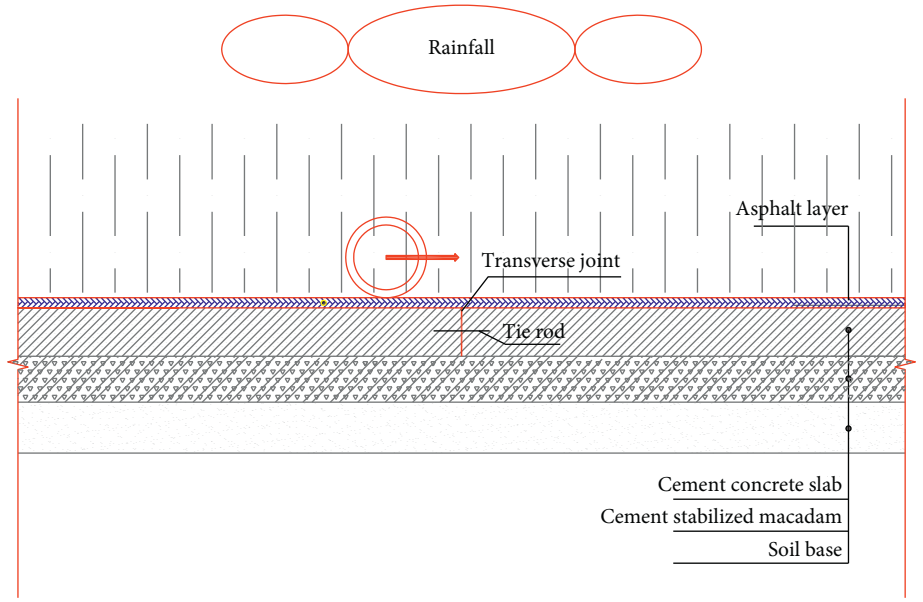

Figure 1: Schematic diagram of a complete pavement structure.

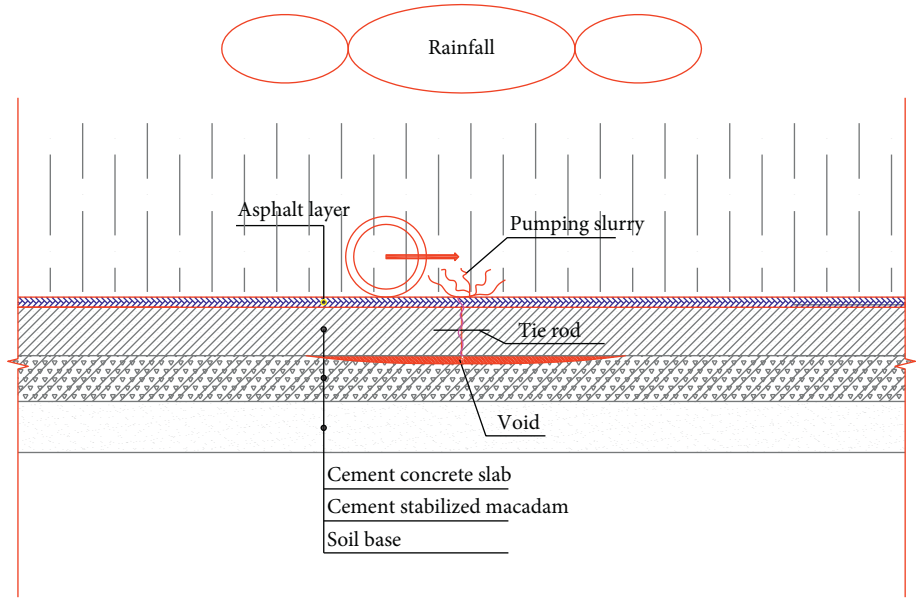

Figure 2: Schematic diagram of a pavement structure with voids.

Figure 3: Actual pavement structure with voids.

Xiao and Li [5]compared the test results of Beckman Beam (BB), Falling Weight Deflectometer (FWD), Ground Penetrating Radar (GPR), and core drilling sampling and proposed to use three indicators to evaluate void, namely, slab corner deflection, midpoint deflection of transverse joint, and joint load transfer coefficient. Xiao [6] took the ratio of joint load transfer efficiency (LTE) to deflection D2 of the loaded slab as an index for evaluating the void and considered that when LTE/D2 < 0.5, the void can be effectively evaluated. Vanden [7] found that loss of support under the slab could be identified even when the joints of the slabs have strong load transfer efficiency. Li et al. [8] used two stress-wave-based techniques, ultrasonic surface wave and impact echo, as well as GPR, to assess the condition of a concrete pavement segment that included a layer of concrete, a granular base, and their interface. Joshaghani and Zollinger [9] examined the relationship between the nondestructive testing data and the actual concrete properties to develop "acceptability of quality" limits. Lai et al. [10] introduced a blind test of nondestructive method for the detection of underground voids below highway pavements using GPR. Miao [11] established an evaluation model of joint load transfer efficiency of cement pavement with and without void, based on the correlation among joint load transfer coefficient, joint stiffness, and void degree. However, that model could not evaluate the void size. Chen and Yin [12] established the relationship between the sum of deflection of a loaded and a nonloaded slab and void size under different values of spring stiffness based on the objective of distinguishing void and load transfer efficiency, so as to evaluate void. Zhang and Xiao [13] proposed a void evaluation method based on the critical load and corresponding deflection in the first load transfer state. Alland et al. [14] developed a statistical classifier to interpret the Falling Weight Deflectometer (FWD) data for the detection of voids under jointed concrete pavement slabs. The void detection methods based on a two-level cross validation process were found to perform better than void detection methods based on variable deflection analyses. Crovetti and Darter [15] developed a graphical void size estimator, which takes into account the normalized corner deflection and the bending corrected LTE to predict the presence of the void and its size. Tong et al. [16] proposed three stages of slab bottom void evolution: the sudden change stage is when the void size is 200–400 mm, the development stage is for void size 400–800 mm, and the accelerated expansion stage is for size 800–1000 mm.

To sum up, there are four commonly used void assessment approaches at present. The first approach includes the deflection values, measured or simulated by FWD or Beckman beam, used for comprehensive evaluation of multiple indices (deflection, deflection difference, load transfer coefficient, etc.) [5]. These evaluation methods aim at a specific project, and when they are used in other projects with different conditions, they are no longer accurate. In the second approach, the deflection basin information measured or simulated by FWD is processed, including slope of deflection basin curve processing, shape variation of void and soil base elastic modulus back calculation. The method [17] for curve processing of deflection basin has limited judgment range and cannot fully reveal the hidden information of deflection basin. Based on the third approach, the evaluation method [11, 12] considers the interaction between the insufficient load transfer capacity of the joints and the void. This kind of method only distinguishes the influence of void and joint load transfer efficiency on deflection to a certain extent through mathematical models, but it does not efficiently involve the change of working law and the change of the joint load transfer system, and it cannot quantitatively evaluate the void. According to the fourth approach, using machine learning evaluation method [16], it is possible to extract more deflection information, but the principle is simple: there are not many factors to take into consideration, and its accuracy is not high.

Hence, the evaluation method of composite pavement slab bottom void should start from the study of joint load transfer mechanism and the in-depth collection of deflection basin information. The major contents of this article are summarized as follows: (1) the spring simulation joint loading algorithm is designed by Python, and the three-dimensional finite element model is established, simultaneously interpreting the different transfer efficiency. (2) Three cases of the change of joint load transfer are analyzed. The main influencing factors and changing rules of the joint transfer capacity are proposed. (3) The influence of the change of joint loading capacity and the void on deflection is determined. The back propagation (BP) neural network algorithm is used to collect information from the deflection basin, and the void evaluation method of composite pavement cement board is proposed. To sum up, this paper adopts a back propagation neural network algorithm to construct the void evaluation method for the first time. In this method, the above four evaluation methods are combined, and a three-way shear spring element is proposed to simulate the load transfer at the joint. Firstly, the FWD model of pavement structure is established to obtain the corresponding deflection basin information. Then, the deflection basin information is sorted out by using the formula. Finally, machine learning is used to evaluate the void. Therefore, this method can distinguish the influence of void and joint load transfer efficiency on deflection and can evaluate quantitatively the void, which cannot be done by other methods.

2. Finite Element Model Description

The three-dimensional finite element model is set up with ABAQUS and C3D8R element is used [18, 19]. The pavement structure layer material is assumed to be isotropic; X, Y, and Z are the driving direction, depth direction, and cross section direction, respectively. The dimensions of the model in X, Y, and Z axes are 10.02 m, 3.00 m, and 5.00 m, respectively. The three-dimensional finite element model with void is shown in Figure 4.

2.1. Determine the Parameters of the Benchmark Model. The parameters of the benchmark model are given in Table 1. In what follows, when the different parameters of Table 1 are

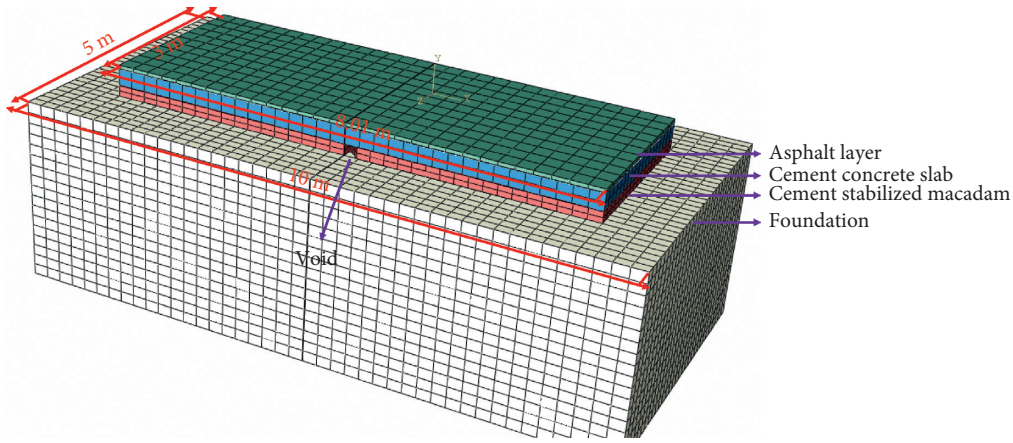

Figure 4: Three-dimensional finite element model with void.

Table 1: Benchmark model parameters.

Structural layer name	Length (m)	Width (m)	Thickness (m)	Elastic modulus (MPa)	Poisson's ratio
Asphalt layer	8.01	3	0.06	2000	0.20
Cement concrete slab	4 * 2	3	0.28	30000	0.15
Cement stabilized macadam	8.01	3	0.18	2600	0.15
Joint width	0.01				
Interlayer state (asphalt layer + cement concrete layer)	The interlayer is smooth				
Interlayer state (cement concrete layer + base course)	The interlayer is completely continuous				

changed, the corresponding factor can be changed on the basis of the benchmark model.

2.2. Simulation Mode of Load Transfer Efficiency

2.2.1. Simulation Method. At present, there are mainly three methods [11] to simulate the load transfer efficiency of cement board joints [6]. Some scientists use three-way shear spring elements. This method requires the calculation of the spring stiffness at each node of the cement concrete slab. This method leads to accurate simulation. Some others set the virtual joint filling material. However, determining the simulation parameters of this material and setting up the finite element requires time-consuming and labor-intensive calculations, as well as high computer performance. Another method is to define the relationship between the two cement contact surfaces as bond slip state. But this method is also computationally expensive to determine the stiffness. In this work, the first method is adopted, using three-way shear spring elements to simulate the dowels of the joint. In this paper, the theoretical method is used to calculate the joint stiffness q. The calculation process is shown in (1)–(7) [11].

$$\mathrm{DCI} = \frac{4\beta^3}{(2+\beta\omega)} E_d I_d, \tag{1}$$

$$\beta = \left(\frac{K\ d}{4E_d I_d}\right)^{1/4}, \tag{2}$$

$$ptC = \frac{E_d I_d}{\omega^3 (1+\phi)}, \tag{3}$$

$$\phi = \frac{12E_d I_d}{G_d A_d \omega^2}, \tag{4}$$

$$G_d = \frac{E_d}{2(1+\mu_d)}, \tag{5}$$

$$D = \frac{1}{(1/DC\ I) + (1/12C)}, \tag{6}$$

$$q = \frac{D}{s}, \tag{7}$$

where E_d is elastic modulus of dowel bar between cement concrete slabs, MPa; I_d is moment of inertia of dowel bar between cement concrete slabs, m^4; K is supporting modulus of concrete to dowel bar, MN/m^3; d is diameter of dowel bar between cement concrete slabs, m; β is relative stiffness of dowel bar concrete, N/m; ω is joint gap width, m; G_d is shear modulus of dowel bar between cement concrete slabs, MPa; A_d is effective cross section area of dowel bar between cement concrete slabs, m^2; μ_d is Poisson's ratio of dowel bar between cement concrete slabs; s is distance between dowel bars and cement concrete slabs, m.

2.2.2. Calculation of Spring Stiffness. Referring to relevant specifications [20–22], the elastic modulus of dowel bar is determined as 200 GPa, Poisson's ratio is 0.3, the diameter of dowel bar is 32 mm, the spacing is 0.3 m, and the joint width is 10 mm, which is a common width for such joints. According to formulae (1)–(7), the calculation results are shown in Table 2.

Table 2: Calculation process of joint stiffness.

Parameter	Units	Calculation results
d	m	0.032
E_d	MPa	2E5
I_d	m^4	5.15×10^{-8}
K_d	MPa	4.07×10^5
ω	m	0.01
β	m^{-1}	23.71
$DC\ I$	$MN \times m^{-1}$	245.45
μ_d	—	0.3
G_d	MPa	76923.08
A_d	m^2	804.2×10^{-4}
ϕ	—	22.19
C	$MN \times m^{-1}$	443.75
D	$MN \times m^{-1}$	234.63
s	m	0.3
q	$MN \times m^{-2}$	782.13

The spring stiffness of the slab corner, slab edge, and slab center is calculated by the formulae (8)–(10), respectively [6]:

$$k_1' = \frac{q \times L}{4 \times (n_r - 1)(n_c - 1)}, \tag{8}$$

$$k_2' = 2 \times k_1', \tag{9}$$

$$k_3' = 4 \times k_1', \tag{10}$$

where k_1' is spring stiffness at cement concrete slab corner, $N \times m^{-1}$; k_2' is spring stiffness at cement concrete slab center, $N \times m^{-1}$; k_3' is spring stiffness at cement concrete slab edge, $N \times m^{-1}$; L is joint length, m; n_r, n_c is number of nodes in rows and columns at the joints on the side of the slab.

The specific arrangement of the springs is shown in Figure 5.

The load transfer diagram at the joint is shown in Figure 6.

2.3. Loading Mode. According to the load equivalent principle, the FWD circular load is simplified as a square load with the side length of 0.266 m [23]. The load is applied directly at the corner of the cement concrete slab, which is the most unfavorable loading position on the slab. The FWD load is simulated as pulse load with a cycle of 30 ms. The maximum load is 0.707 MPa.

The ratio of vertical displacement (deflection) of both sides of joint of the adjacent concrete slabs is defined as deflection load transfer coefficient. The cement concrete slab directly under the load is referred to as the loaded slab, and the adjacent slab is referred to as the nonloaded slab.

3. Research Plan

With the cyclic traffic load and the influence of external environment, the load transfer efficiency of cement concrete slab will eventually degrade. In general, the strength degradation of cement concrete material results in the reduction of load transfer efficiency of cement concrete slab. The void problem does not occur when the strength of the base is high. However, the strength of the foundation gradually decreases under long-term loading, and spalling can be observed on the top surface of the base. After that, voids appear at the bottom of the slab, which aggravates the reduction of the load transfer efficiency. In some special cases, due to mistakes during construction period, some voids are created at the bottom of the cement concrete slab. In such a case, the load transfer efficiency may be in accordance with the design requirements, but in long term the cement concrete slab breaks or the dowels are pulled out. At that time, the load transfer efficiency is dramatically reduced.

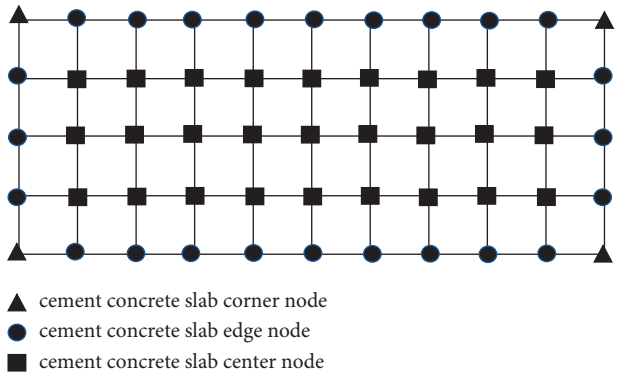

Figure 5: Schematic diagram of nodes of cement concrete slab.

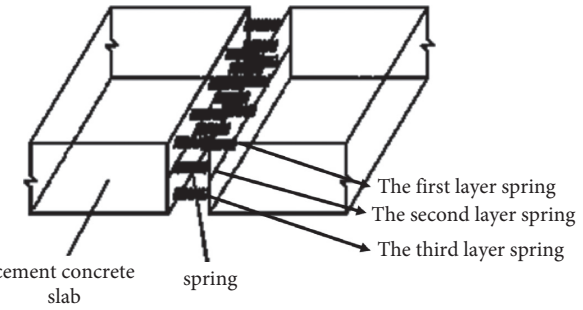

Figure 6: Schematic diagram of using spring to simulate load transfer at the joint.

In view of the three situations that cause the decrease of load transfer efficiency, the research scheme of this work is as follows. Firstly, on the basis of the benchmark model, the influence of structural parameters, such as spring stiffness and contact laws between layers, on the load transfer efficiency of joints is analyzed. Grey correlation and sensitivity analyses are used to determine the main influential factors. Finally, the influence of void type and size on the load transfer efficiency of joint under different spring stiffness is determined.

4. Variation of Load Transfer Efficiency of Cement Concrete Slab Joints without Voids

The influence of six factors on the load transfer efficiency of the joint of the nonvoid cement concrete slab is considered, including the elastic modulus of the foundation ground

(150 MN/m^3, 75MN/m^3, 100MN/m^3, 200 MN/m^3, 400 MN/m^3), the friction coefficient between layers (0, 0.3, 0.5, 0.7, 1.0), the elastic modulus of the asphalt layer (200 MPa, 500 MPa, 1000 MPa, 2000 MPa, 4000 MPa, and 10000 MPa), and its thickness (2 cm, 4 cm, 6 cm, 12 cm, 16 cm, and 20 cm), as well as the elastic modulus of the cement concrete slab (20000 MPa, 25000 MPa, 30000 MPa, 35000 MPa, and 40000 MPa) and its thickness (20 cm, 22 cm, 24 cm, 26 cm, 28 cm, and 30 cm) under different spring stiffness (0.01 q, 0.1 q, q, 10 q, and 100 q). Based on formulae (8)–(10), the values of the joint stiffness at different points of the slab are given in Table 3.

4.1. Influence of Asphalt Layer Elastic Modulus on Deflection Load Transfer Coefficient. The calculation results of deflection load transfer coefficient of cement concrete slab under different spring stiffness and asphalt layer elastic moduli are shown in Figure 7.

When the spring stiffness is smaller than 0.1 q, the deflection load transfer coefficient slightly increases with the increase of asphalt layer elastic modulus. For such values of springs, the deflection load transfer coefficient is about 76%. However, when the spring stiffness is larger than 0.1 q, the deflection load transfer coefficient gradually decreases with the increase of asphalt layer elastic modulus with values that vary between 93% and 89%. When the spring stiffness exceeds q, the deflection load transfer coefficient is larger than 94%, which means that 94% of the load is transferred from one side of the joint to the other.

Under the same spring stiffness, increasing the asphalt layer elastic modulus has limited influence on the deflection of the slabs. Hence, using an asphalt material with increased elastic modulus will not lead to a sufficient increase of the deflection load transfer coefficient of cement concrete slab.

4.2. Influence of Asphalt Layer Thickness on Deflection Load Transfer Coefficient. The calculation results of deflection load transfer coefficient of cement concrete slab under different values of spring stiffness and asphalt layer thicknesses are shown in Figure 8.

With the increase of asphalt layer thickness, the deflection load transfer coefficient gradually increases when the spring stiffness is small, but it remains almost the same for stiffness coefficient equal or larger than q.

When the spring stiffness is equal or larger than q, the deflection load transfer coefficient is larger than 95%; when the spring stiffness ≥0.1 q, the deflection load transfer coefficient is larger than 85%; when the spring stiffness = 0.01 q, the deflection load transfer coefficient is about 76%.

When the spring stiffness decreases from 10 q to q and the thickness of asphalt layer is larger than 4 cm, the deflection load transfer coefficient of the two is almost the same, but when the spring stiffness is reduced from q to 0.01 q, the deflection load transfer coefficient drops sharply.

4.3. Influence of Cement Concrete Slab Elastic Modulus on Deflection Load Transfer Coefficient. The calculation results of deflection load transfer coefficient under different values of spring stiffness and cement concrete slab elastic moduli are shown in Figure 9.

The deflection load transfer coefficient decreases with the increase of the elastic modulus of the cement concrete slab, for spring stiffness smaller than 100 q. When the spring stiffness is equal or larger than q, the deflection load transfer coefficient is larger than 94%; when the spring stiffness ≥0.1 q, the deflection load transfer coefficient is greater than 87%; when the spring stiffness = 0.01 q, the deflection load transfer coefficient is about 73%.

The larger the spring stiffness, the smaller the influence of the elastic modulus of cement concrete slab on the deflection load transfer coefficient. When the spring stiffness is equal or larger than 10 q, any change of the elastic modulus of the cement concrete slab has no effect on the deflection load transfer coefficient; when the spring stiffness ≤0.1 q, the deflection load transfer coefficient decreases linearly with the increase of the elastic modulus of the cement concrete slab.

4.4. Influence of Thickness of Cement Concrete Slab on Deflection Load Transfer Coefficient. The calculation results of deflection load transfer coefficient of cement concrete slab with different spring stiffness and thicknesses of cement concrete slab are shown in Figure 10.

It is noted that when the spring stiffness is constant, the deflection load transfer coefficient decreases with the increase of the thickness of the cement concrete slab. This reduction is smaller for large values of spring stiffness. When the spring stiffness ≥q, the deflection load transfer coefficient is larger than 95%; when the spring stiffness ≥0.1 q, the deflection load transfer coefficient is larger than 89%; when the spring stiffness = 0.01 q, the deflection load transfer coefficient is about 74%.

The larger the spring stiffness, the smaller the influence of the thickness of cement concrete slab on the deflection load transfer coefficient. When the spring stiffness ≥q, the increase of the thickness of the cement concrete slab has small effect on this coefficient; when the spring stiffness = 0.01 q, it decreases linearly with the increase of the thickness of the cement concrete slab.

4.5. Influence of Elastic Modulus of the Foundation Ground on Deflection Load Transfer Coefficient. The calculation results of deflection load transfer coefficient of cement concrete slab under different values of spring stiffness and ground elastic moduli are shown in Figure 11.

The deflection load transfer coefficient decreases with the increase of the elastic modulus of the foundation ground. When the spring stiffness is equal or larger than 10 q, the deflection load transfer coefficient is larger than 92%.

The smaller the spring stiffness is, the larger the influence of the modulus of foundation ground on the deflection load transfer coefficient is. When the spring stiffness ≤0.1 q and the foundation ground modulus ≥100 MN/m^3, the deflection load transfer coefficient decreases with the increase of ground elastic modulus. The reason is that when the foundation strength is enhanced (increased modulus), the

Table 3: Joint stiffness at different points of the slab.

Different spring stiffness application number	Spring stiffness at cement concrete slab corner ($N \times m^{-1}$)	Spring stiffness at cement concrete slab center ($N \times m^{-1}$)	Spring stiffness at cement concrete slab edge ($N \times m^{-1}$)
0.01 q	1.5×10^5	3.0×10^5	6.0×10^5
0.1 q	1.5×10^6	3.0×10^6	6.0×10^6
q	1.5×10^7	3.0×10^7	6.0×10^7
10 q	1.5×10^8	3.0×10^8	6.0×10^8
100 q	1.5×10^9	3.0×10^9	6.0×10^9

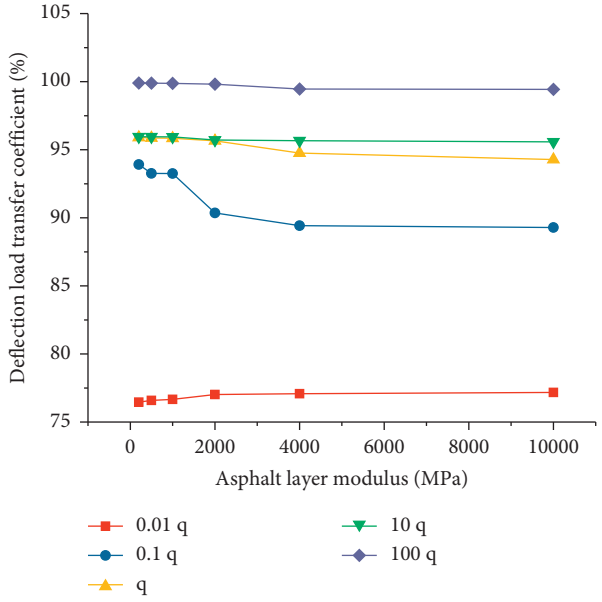

Figure 7: Variation of deflection load transfer coefficient with respect to the asphalt layer elastic modulus under different values of spring stiffness.

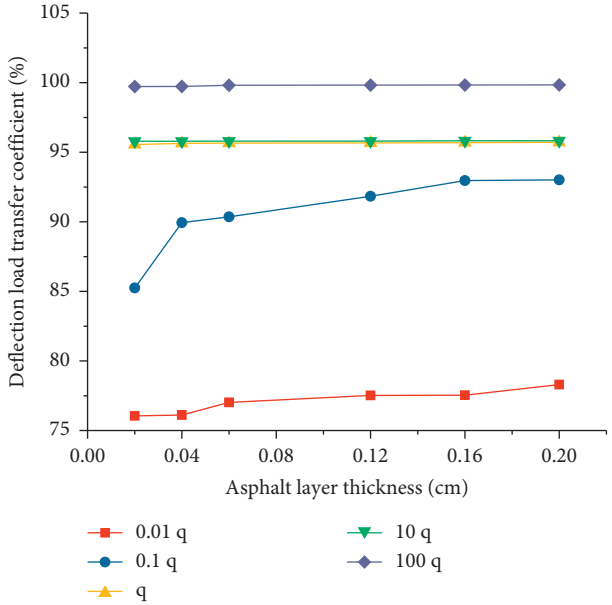

Figure 8: Variation of deflection load transfer coefficient with respect to the asphalt layer thickness under different values of spring stiffness.

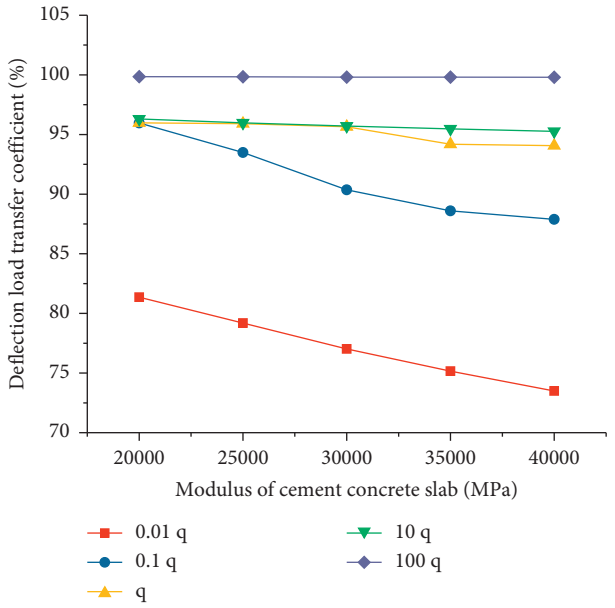

Figure 9: Variation of deflection load transfer coefficient with respect to the elastic modulus of cement concrete slab under different values of spring stiffness.

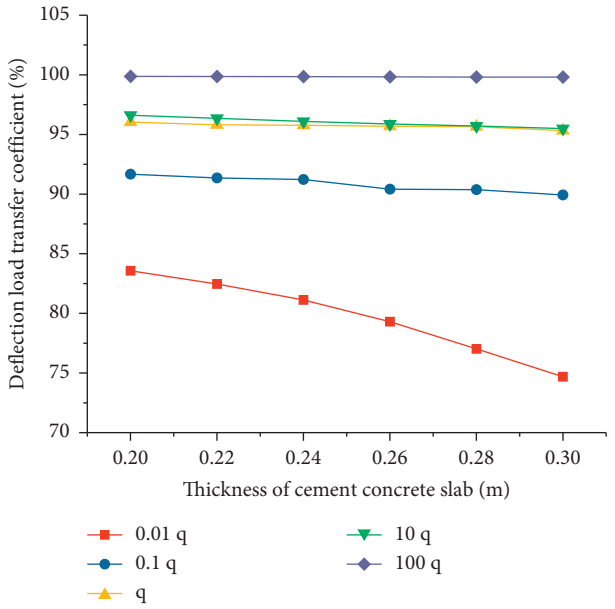

Figure 10: Variation of deflection load transfer coefficient with respect to the thickness of cement concrete slab under different values of spring stiffness.

load will be more widely distributed to the foundation, the load of the nonloaded slab will be reduced, and the corresponding deflection load transfer coefficient will be reduced.

4.6. Influence of Interlayer Friction Coefficients on Deflection Load Transfer Coefficient. The calculation results of deflection load transfer coefficient of cement concrete slab with different values of spring stiffness and interlayer friction coefficients are shown in Figure 12.

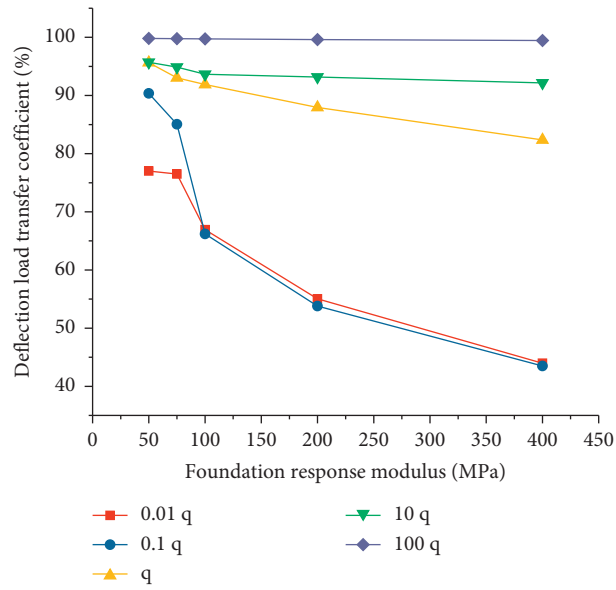

Figure 11: Variation of deflection load transfer coefficient with respect to the elastic modulus of the foundation ground under different values of spring stiffness.

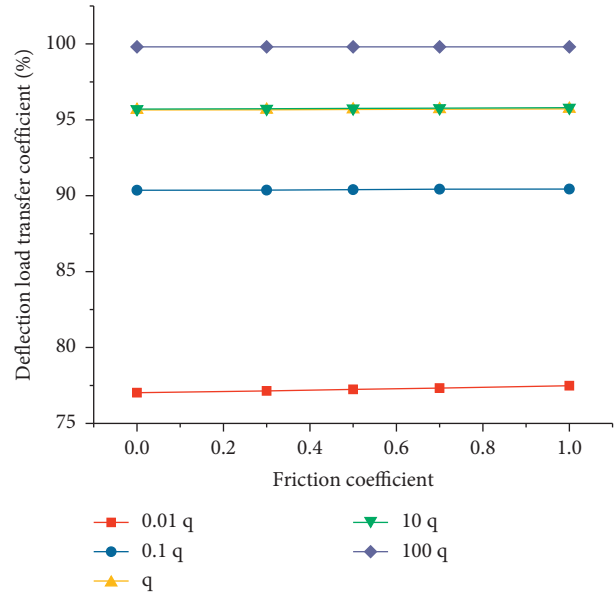

Figure 12: Variation of deflection load transfer coefficient with respect to friction coefficient under different values of spring stiffness.

With the increase of friction coefficient, the coefficient of deflection load transfer remains almost unchanged. When the friction coefficient increases from 0 to 1, the deflection load transfer coefficient increases from 77.02%, 90.36%, 95.65%, 95.71%, and 99.81% to 77.48%, 90.44%, 95.72%, 95.80%, and 99.81% under the spring stiffness of 0.01 q, 0.1 q, 10 q, and 100 q, respectively. Therefore, the friction coefficient has no effect on the deflection load transfer coefficient of cement concrete slab.

In this paper, "spring stiffness" is used to reflect the strength of joint filling material between the cement concrete

slabs. The larger the strength of the filler material is, the larger the spring stiffness is and the stronger the adhesion between the slabs is. From Figures 7–12, it can be seen that the deflection load transfer coefficient of spring stiffness q is very close to that of 10 q. This indicates that in the design of pavement structure, the spring stiffness can meet the design requirements (means q). It is unnecessary to increase the spring stiffness by increasing the strength of the joint filling material, because even if the spring stiffness is increased to 10 q, the deflection load transfer coefficient will not increase as the stress between cement concrete slabs will not be greatly improved. The deflection load transfer coefficient will increase for larger spring stiffness, up to 100 q, but from the perspective of construction cost, this is not even realistic.

4.7. Correlation Degree and Sensitivity Analysis of Influencing Factors of Deflection Load Transfer Coefficient Based on Grey Theory. In order to determine the influence degree of the studied parameters on the deflection load transfer coefficient, the importance of the six factors is analyzed by Grey Correlation Degree Theory.

Considering the deflection load transfer coefficient and different values of spring stiffness as evaluation indices, interlayer friction coefficient, modulus of foundation ground, thickness of cement concrete slab, cement concrete slab elastic modulus, asphalt layer thickness, and asphalt layer elastic modulus are selected as the comparison sequence indices.

Based on Table 4, it can be seen that the influence degree of each factor on the deflection load transfer coefficient is almost the same under different values of spring stiffness, and the order is modulus of foundation ground > asphalt layer thickness > cement concrete slab elastic modulus > thickness of cement concrete slab > asphalt layer elastic modulus > interlayer friction coefficient.

The sensitivities of the six factors to the deflection load transfer coefficient are analyzed. The calculation results are shown in Table 5.

For the deflection load transfer coefficient, the sensitivity order of the six factors is modulus of foundation ground > cement concrete slab elastic modulus > asphalt layer elastic modulus > asphalt layer thickness > thickness of cement concrete slab > interlayer friction coefficient.

In conclusion, it is noted that the modulus of foundation ground has the greatest influence on the joint load transfer and the interlayer friction coefficient has the smallest.

5. Analysis of Load Transfer Efficiency of Cement Concrete Slab Joints with Voids

Due to mistakes during construction period, some voids are often created at the bottom of the cement concrete slab. In such a case, the load transfer efficiency may be in accordance with the design requirements. In order to investigate this case, the prism with isosceles right-angle triangle is adopted to simulate the void shape. The prism has the same height as the base, and four different side lengths of the triangle are assumed (called void size), namely 0.2 m, 0.4 m, 0.8 m, and 1 m, respectively.

The cement stabilized macadam elastic modulus is reduced to simulate the degree of void. Taking the elastic modulus of 0 MPa, 650 MPa, 1300 MPa, 1950 MPa, and 2600 MPa, the degree of void is 1, 0.75, 0.5, 0.25, and 0, respectively. For example, the cement stabilized macadam elastic modulus is 2600 MPa, indicating that there are no voids below the pavement, so the degree of void = 0 (no void). Two types of void forms are selected, i.e., semi- and full void at slab corner. The semivoid refers to the void under the loaded cement concrete slab. The full void means that there is void under both loaded and nonloaded slabs, and the shape of the void is the same for both slabs. The calculation results of different combinations of working conditions are shown in Table 6.

Based on Table 6, it can be noted that under the same conditions, the deflection load transfer coefficient of semivoid at the slab corner is larger than the one of full void, and the larger the degree of void is, the smaller the deflection load transfer coefficient is, indicating that further development of void could lead to a poor load transfer efficiency.

With the increase of void size and degree, the deflection of the loaded and nonloaded slab gradually increases, resulting in small change of deflection load transfer coefficient.

When the void degree increases from 0.75 to 1, the deflection value increases sharply and the deflection increase rate changes abruptly. When the void degree is smaller than 0.75, the deflection value of different void degree presents small difference. Taking the void size of 0.2 m as an example, when the void degree increases gradually from 0, 0.25, 0.5, 0.75, and 1, the increase rates of deflection difference corresponding to semivoid are 1.2%,3.4%,16.3%, and 43.2%, respectively, and those corresponding to full void are 3.5%, 16.5%, 17.6%, and 41.0%, respectively. When the void degree is 1 and the void size increases gradually from 0.2, 0.4, 0.8, and 1, the increase rate of deflection difference corresponding to semivoid is 3.5%, 8.5%, 24.8%, and 45.2%, respectively, and the one of full void is 13.7%, 15.8%, 17.8%, and 46.7%, respectively.

Therefore, when there is no base under the cement concrete slab, that is, when there is complete void (void degree = 1), the deflection load transfer coefficient of cement concrete slab is 80%, which will lead to unstable stress of the pavement structure and consequently to pavement collapse. However, when there is no complete void (void degree = 0.25, 0.5, 0.75), the spring can effectively restrain the deformation of cement concrete slab and protect the stability of the pavement.

6. Variation Law of Joint Load Transfer Efficiency under Interaction of Void and Spring Stiffness

Based on the analysis of the cement concrete slab joints with voids, presented in the previous section, it can be noted that the deflection increases with the increase of the size and degree of the void, and the void has an interactive effect on the load transfer efficiency. Assuming that there is no base under the cement concrete slab, that is, when there is

Table 4: Correlation between reference sequence and contrast sequence.

Correlation degree		Interlayer friction coefficient	Asphalt layer elastic modulus	Modulus of foundation ground	Asphalt layer thickness	Cement concrete slab elastic modulus	Thickness of cement concrete slab
Deflection load transfer coefficient	0.01 q	0.930	0.956	0.986	0.985	0.962	0.959
	0.1 q	0.928	0.955	0.984	0.983	0.961	0.957
	q	0.936	0.960	0.992	0.991	0.968	0.965
	10 q	0.938	0.960	0.994	0.993	0.969	0.967
	100 q	0.939	0.961	0.995	0.994	0.970	0.968

Table 5: Sensitivity analysis.

Correlation degree		Interlayer friction coefficient	Modulus of foundation ground	Thickness of cement concrete slab	Cement concrete slab elastic modulus	Asphalt layer thickness	Asphalt layer elastic modulus
Deflection load Transfer coefficient	0.01 q	0.0117	1.2776	0.0484	0.1985	0.0694	0.2246
	0.1 q	0.0016	1.9045	0.0332	0.2080	0.1540	0.2123
	q	0.0052	1.3947	0.0167	0.1396	0.1258	0.1986
	10 q	0.0202	1.8070	0.0081	0.2337	0.1270	0.2517
	100 q	0.0000	1.3067	0.1064	0.1368	0.1277	0.3957

Table 6: Deflection values of loaded and nonloaded cement concrete slabs under different void characteristics.

Void degree	Void size/ m	Semivoid at slab corner				Full void of slab corner			
		Loading slab/ 0.01 mm	Nonloaded slab/ 0.01 mm	Deflection difference/ 0.01 mm	Deflection load transfer coefficient%	Loading slab/ 0.01 mm	Nonloaded slab/ 0.01 mm	Deflection difference/ 0.01 mm	Deflection load transfer coefficient%
1	1	11.56	9.29	2.28	80.4	12.58	9.96	2.61	79.2
	0.8	11.31	9.09	2.22	80.4	12.20	9.61	2.59	78.8
	0.4	10.59	8.65	1.94	81.7	11.14	8.80	2.34	79.0
	0.2	10.31	8.48	1.83	82.3	10.70	8.59	2.12	80.3
0.75	1	10.07	8.82	1.25	87.6	10.25	8.86	1.39	86.4
	0.8	10.00	8.75	1.25	87.5	10.14	8.85	1.29	87.3
	0.4	9.89	8.65	1.24	87.5	9.95	8.68	1.27	87.2
	0.2	9.79	8.75	1.04	89.4	9.81	8.56	1.25	87.3
0.5	1	9.73	8.79	0.94	90.3	9.76	8.56	1.20	87.7
	0.8	9.64	8.73	0.91	90.6	9.71	8.62	1.09	88.8
	0.4	9.59	8.70	0.89	90.7	9.69	8.66	1.04	89.4
	0.2	9.57	8.70	0.87	90.9	9.65	8.63	1.03	89.4
0.25	1	9.55	8.69	0.86	91.0	9.58	8.57	1.01	89.5
	0.8	9.51	8.66	0.85	91.1	9.53	8.59	0.95	90.1
	0.4	9.46	8.62	0.84	91.1	9.49	8.58	0.91	90.4
	0.2	9.44	8.60	0.84	91.1	9.47	8.62	0.86	91.0
0	—	9.29	8.45	0.83	91.0	9.29	8.45	0.83	91.0

complete void (void degree = 1), the influence of spring stiffness and void size on the load transfer efficiency of the joint is analyzed. The values of spring stiffness for the different points of the slab are given in Table 7.

6.1. Variation Law of Load Transfer Efficiency of Joints. The maximum deflection values of loaded and nonloaded cement concrete slab are calculated and presented in Figure 13. The deflection load transfer coefficient under different values of spring stiffness and degree of void are given in Tables 8, 9.

With the increase of spring stiffness, the deflection of loaded and nonloaded slabs decreases, and with the increase of void degree, the deflection of both slabs increases. When the spring stiffness is equal or smaller than 0.1 q, the deflection increases nonlinearly with the increase of the void degree.

With the increase of spring stiffness, the deflection load transfer coefficient generally decreases and the larger the void degree, the smaller the reduction of the deflection load transfer coefficient. When the spring stiffness is larger than 0.1 q, the deflection load transfer coefficient shows a small change. The larger the void size is, the smaller the deflection load transfer coefficient is. This occurs because with the increase of spring stiffness, the loaded slab will bear more load, resulting in larger deformation and smaller deflection load transfer coefficient. Therefore, if the spring stiffness is too large, it will be unfavorable to load transfer; at the same time, if the spring stiffness is too small, such as <0.1 q,

Table 7: Spring stiffness at different points of the slab.

Different spring stiffness application number	Cement concrete slab corner/ $N \times m^{-1}$	Cement concrete slab center/ $N \times m^{-1}$	Cement concrete slab edge/ $N \times m^{-1}$
0.005q	8.25×10^4	1.65×10^5	3.3×10^5
0.01q	1.5×10^5	3.0×10^5	6.0×10^5
0.05q	8.25×10^5	1.65×10^6	3.3×10^6
0.1q	1.5×10^6	3.0×10^6	6.0×10^6
0.5q	8.25×10^6	1.65×10^7	3.3×10^7
q	1.5×10^7	3.0×10^7	6.0×10^7
5q	8.25×10^7	1.65×10^8	3.3×10^8
10q	1.5×10^8	3.0×10^8	6.0×10^8

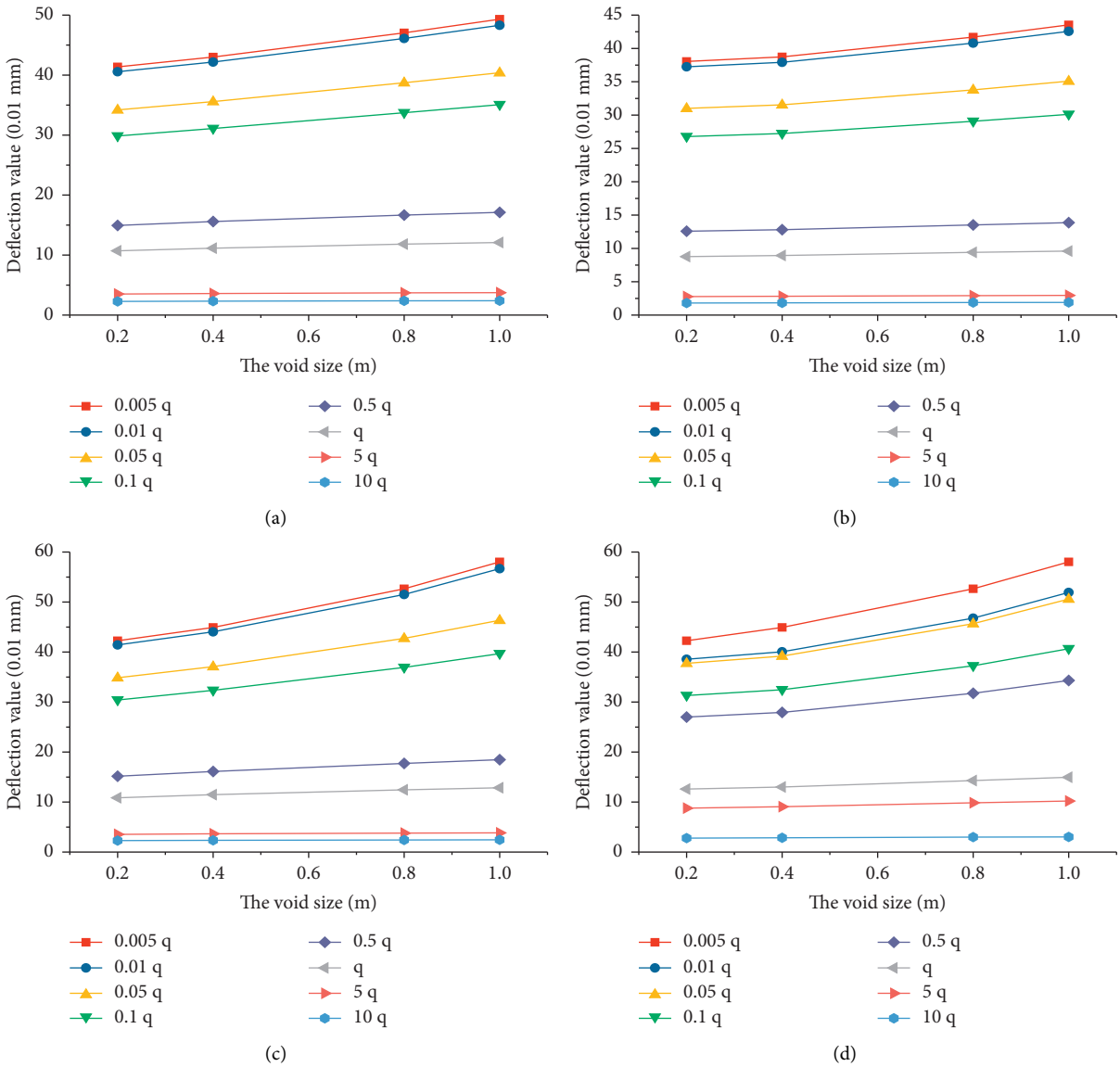

Figure 13: Slab deflection under different values of spring stiffness and degree of void: (a) deflection of loaded slab with semivoid state, (b) deflection of nonloaded slab with semivoid state, (c) deflection of loaded slab with full void state, and (d) deflection of nonloaded slab with full void state.

although the deflection load transfer coefficient is large, the pavement structure deformation is very large, which is unfavorable for the cement concrete slab. Therefore, the spring stiffness should be in the range of 0.5 q–5 q.

6.2. Interaction Mechanism between Joint Load Transfer Efficiency and Void Separation. Figure 13 and Tables 8, 9 show that the deflection of the loaded and nonloaded slab is larger when full voids exist at the bottom of the slab. When the

Table 8: Deflection load transfer coefficient under different values of spring stiffness and degree of void (semivoid state).

Void size (m)	Spring stiffness							
	0.005 q (%)	0.01 q (%)	0.05 q (%)	0.1 q (%)	0.5 q (%)	q (%)	5 q (%)	10 q (%)
0.2	92	92	91	90	84	82	79	79
0.4	90	90	89	88	82	80	79	79
0.8	89	88	87	86	81	79	79	80
1	88	88	87	86	81	79	79	80

Table 9: Deflection load transfer coefficient under different values of spring stiffness and degree of void (full void state).

Void size (m)	Spring stiffness							
	0.005 q (%)	0.01 q (%)	0.05 q (%)	0.1 q (%)	0.5 q (%)	q (%)	5 q (%)	10 q (%)
0.2	91	91	90	89	83	81	79	79
0.4	89	89	88	86	81	79	78	79
0.8	89	89	87	86	81	79	79	79
1	89	89	88	86	81	79	79	80

spring stiffness is larger than q, the load transfer coefficient of half and full void is about 80%, and there is no change with the increase of void size. It can be seen that the influence of spring stiffness on deflection and deflection load transfer coefficient is complex. Therefore, when the degree of void is 1, semi- and full void are compared and analyzed by means of the force conditions of the three-layer spring with transverse and longitudinal seams under different void forms, as shown in Figures 14, 15.

The force direction of the spring arranged in the driving direction is in Y direction, as shown in Figure 15(a); the force direction of the spring arranged in the cross sectional direction is in X direction, as shown in Figure 15(b). In Figure 15(a), the abscissa is the displacement from the midline of the transverse seam, while, in Figure 15(b), the abscissa is the displacement from the midline of the longitudinal seam. It is agreed that the displacement of the spring towards the center line on the loaded slab is negative, and the one towards the center line on the nonloaded slab is positive.

The mechanical distribution law of the spring along the cross section at the longitudinal seam is not the same for all layers. The first layer spring is mainly subjected to tension at the top surface of the cement slab. The third layer spring is mainly subjected to compression at the bottom surface of the cement slab. The second layer spring is in the alternating state between tension and compression. The mechanical distribution law of the first and third layer springs follows an approximate parabolic distribution. Similarly, the mechanical distribution law of the spring at the transverse seam along the driving direction depends on the spring layers. The first and third layer springs of the cement slab have a hyperbolic distribution form, but the direction is opposite. The second layer spring is in the state of alternating tension and compression. The first layer of spring at the top surface of the loaded cement slab is mainly subjected to tension, and the third one is mainly subjected to compression. The first layer spring of the nonloaded slab is mainly under compression, and the third one is mainly under tension. It can be seen that the spring in the void area is in the torsional shearing state when the void exists.

The mechanical behaviors of the springs in the two different directions show that the force of the spring near the void area is large, and the force of the spring far away from the void area is small and gradually tends to zero; Figure 15 shows that all springs do not work at the same time, but some springs near the void area participate in the work when resisting the pavement deformation caused by the void. When the spring near the void area "yields" and fails, a large range of springs begin to work together.

7. Void Evaluation Method of Composite Pavement Cement Concrete Slab

The load transfer of joints is not comprehensive in considering in the current research, so a more accurate void evaluation method is obtained. The analysis scheme in Section 3 distinguishes the decrease of spring stiffness caused by the void at the bottom of slab from the one caused by the decay of the road structure. Therefore, based on the above classification analysis conclusion, a large number of finite element calculations are carried out considering the joint load transfer and voids. The BP neural network algorithm is used to derive information from the deflection basin, and the void evaluation method of composite pavement cement concrete slab is proposed.

A small size of void is more difficult to be identified. Therefore, the setting of void size can be divided into the following three situations: no void, 0.2 m and 0.4 m. There are two forms of void: semi- and full void at the bottom of slab. The spring stiffness is set as 0.005 q, 0.01 q, 0.05 q, 0.1 q, 0.5 q, q, 5 q, and 10 q; at the same time, soil elastic modulus is set as 40 MPa, 80 MPa, 100 MPa, and 200 MPa (in order to simplify the calculation and reduce the workload), a total of 160 pavement conditions to form a database.

The research ideas are as follows. Firstly, the working condition of FWD in pavement deflection measurement is simulated by finite element method, and the pavement deflection basin data are obtained (the curve of deflection measured by FWD at different positions is called pavement deflection basin, which contains rich pavement structure

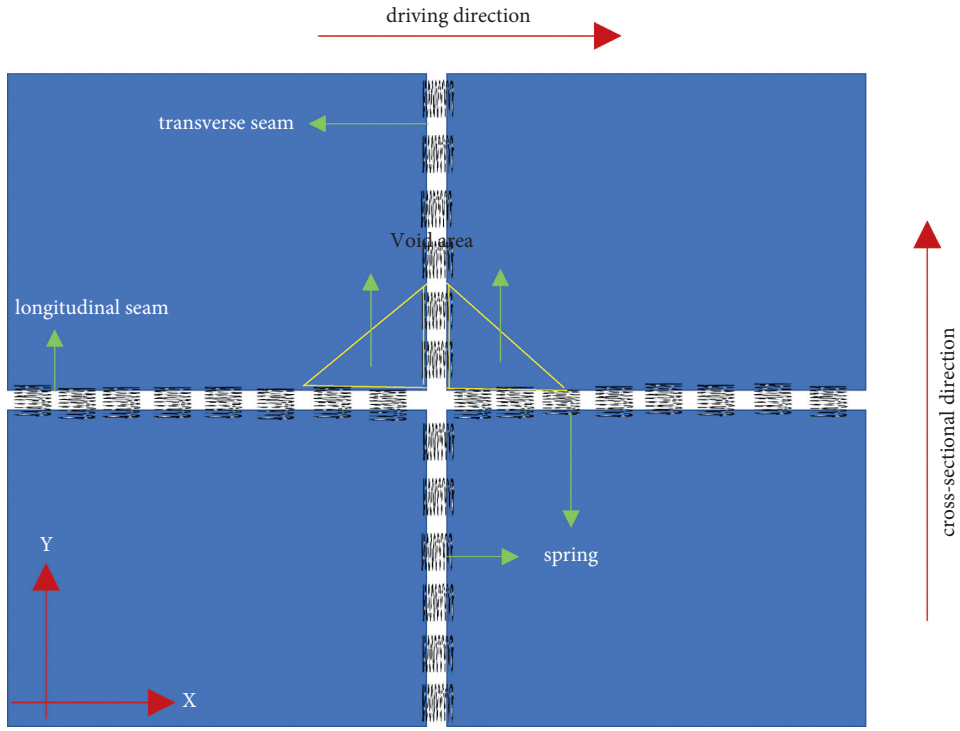

Figure 14: Cement concrete slab spring plan.

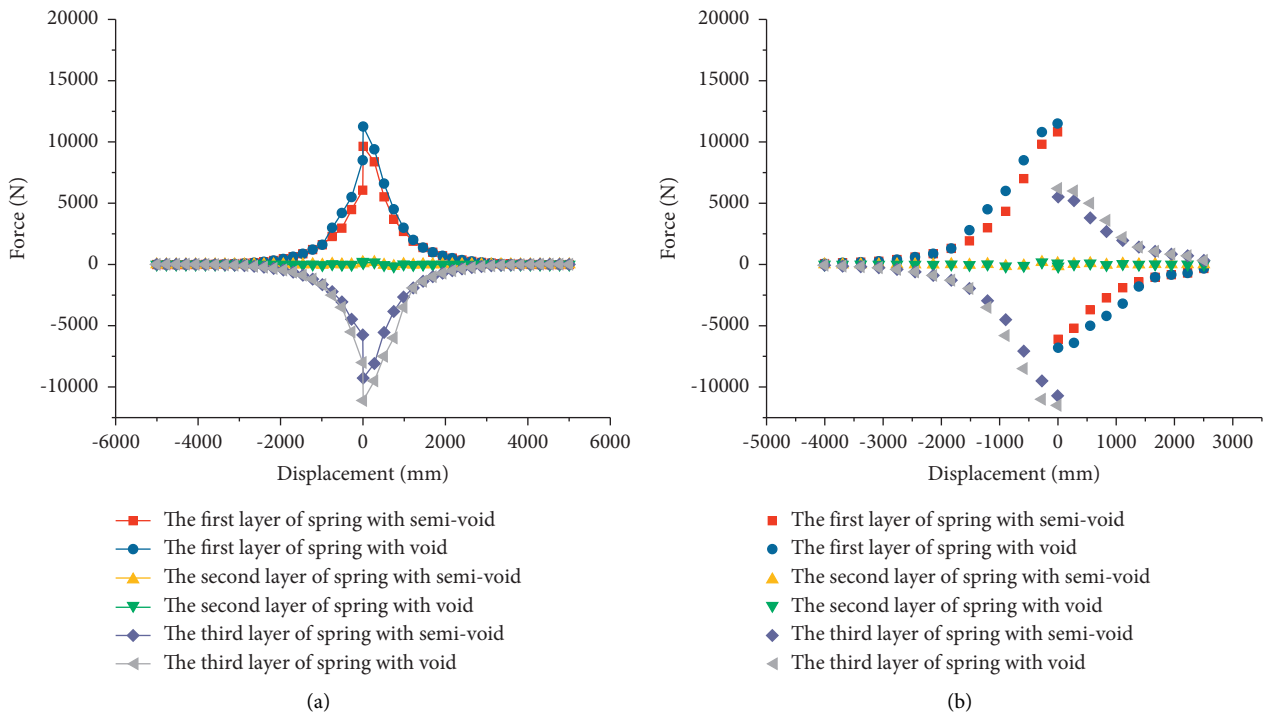

Figure 15: (a) Force analysis of three-layer spring in driving direction. (b) Force analysis of three layer spring in cross-sectional direction.

information and can be used for void evaluation [24, 25]). In addition, the ($y = ae^{bx}$) is used to fit the pavement deflection basin data. Parameters a and b, obtained by fitting, are used as the input parameters of neural network simulation fitting. Finally, the actual test data of FWD are brought into the BP neural network to establish the void evaluation method, and the spring stiffness, void size, and soil elastic modulus are determined.

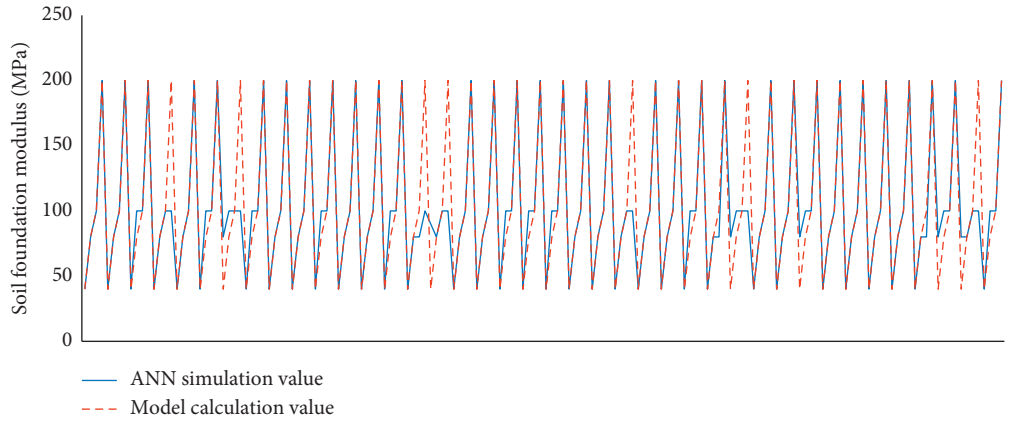

Figure 16: Fitting effect of soil foundation elastic modulus.

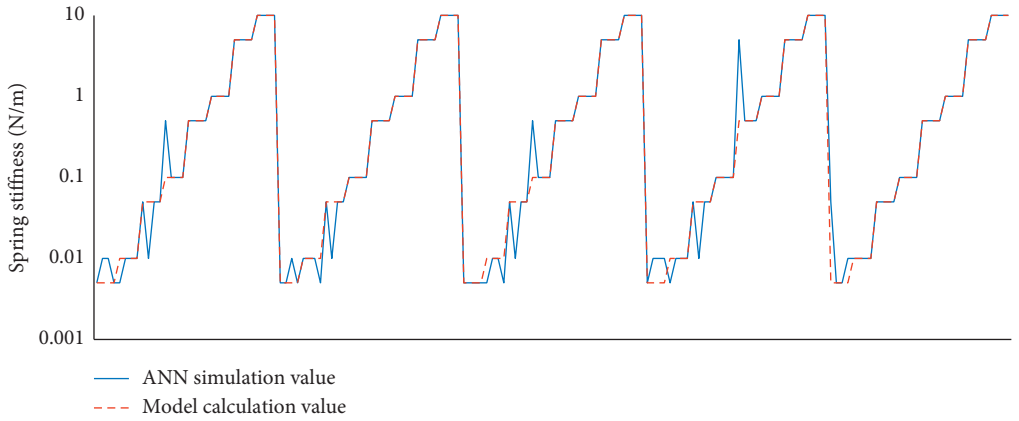

Figure 17: Fitting effect of spring stiffness.

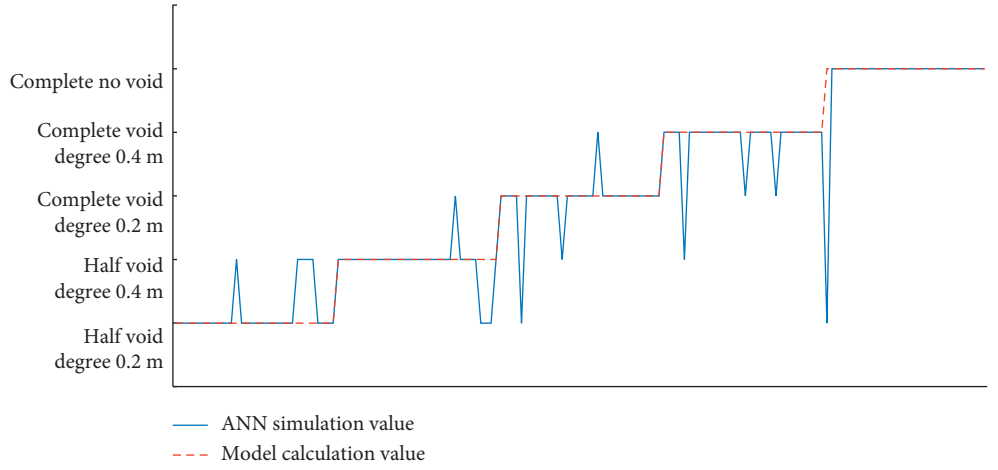

Figure 18: Fitting effect of void degree.

7.1. Establish Void Evaluation Method by Using Neural Network. For 160 groups of model calculation values, 70% (112 groups) are randomly selected as the training data set of the model, 15% (24 groups) are randomly selected as the verification data set of the model, and 15% (24 groups) are randomly selected as the test data set of the model [26]. There are 15 hidden layers in the neural network, and the training algorithm is Bayesian regularization [27, 28].

The simulation results of soil foundation elastic modulus, spring stiffness, and void degree are obtained through

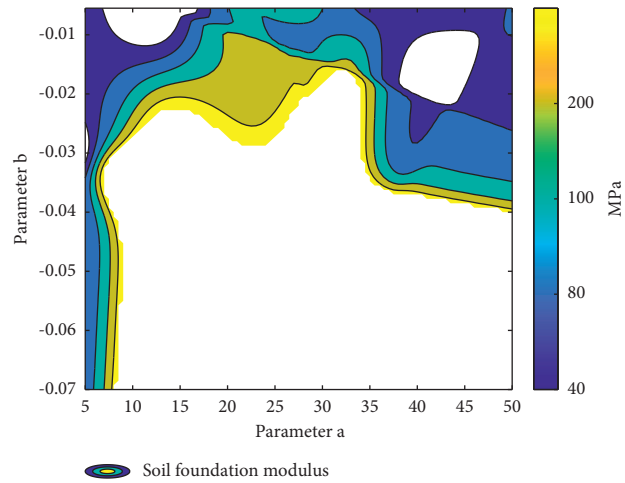

Figure 19: Values of parameters a and b under different soil foundation elastic modulus.

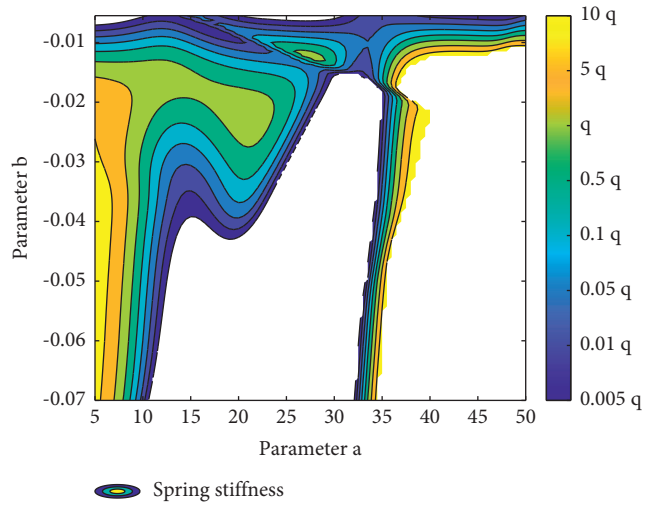

Figure 20: Values of parameters a and b under different spring stiffness.

the comprehensive evaluation model of neural network, as shown in Figures 16–18, where ANN corresponds to the fitting data. It can be seen that the model can get the corresponding soil modulus, spring stiffness, and void degree according to the parameters *a* and *b* fitted. The correlation coefficient of the model is 0.923 for soil modulus, 0.985 for spring stiffness, and 0.942 for void degree.

Based on the above comprehensive model, the soil foundation modulus, spring stiffness, and void degree corresponding to different parameters a and b are obtained, as shown in Figures 19–21, where the horizontal and vertical-left axes show the values of parameters a and b, respectively, while the vertical-right axis shows the change of the studied magnitudes with respect of a and b. When parameter a increases from 5 to 15, the soil foundation elastic modulus shows an increasing trend. The influence of parameter b on the change of soil foundation elastic modulus is small. When parameter a is larger than 15, the change of soil foundation elastic modulus is mainly affected by parameter b, and with the increase of parameter b, the soil foundation elastic modulus shows a decreasing trend. Parameter a has significant influence on the spring stiffness in the range of 5–10 and 30–35. More specifically, the spring stiffness decreases with the increase of parameter a varying between 5 and 10, and it increases with the increase of parameter a between 30 and 35. When parameter a varies between 15 and 30, the spring stiffness first increases and then decreases with the increase of parameter b. When parameter a is in the range of 35–50, the spring stiffness increases with the increase of parameter b.

In conclusion, the void evaluation process of composite pavement is as follows. Firstly, FWD is used to carry out the first level void evaluation loading. In addition, the exponential curve is used to fit so as to get the values of parameters a and b. Finally, based on Figures 19–21, the ground elastic modulus, spring stiffness, and void form of the composite pavement are determined.

7.2. Actual Engineering Verification. The data of Weixu Expressway void were detected in August 2018. They are given in Table 10, while the field FWD is shown in Figure 22.

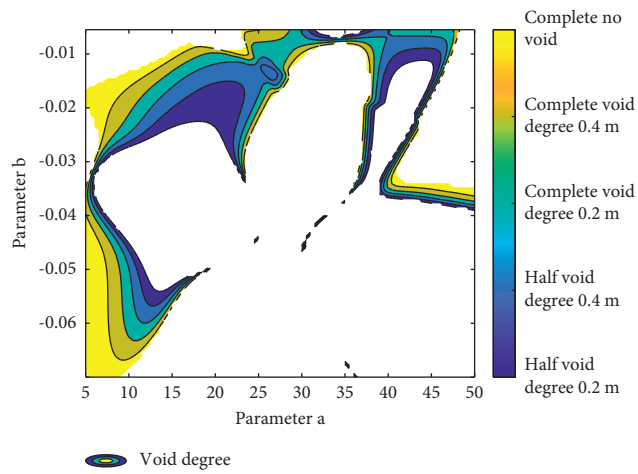

Figure 21: Values of parameters a and b under different void degrees.

Table 10: Deflection value detection of first stage loading in void section.

Serial number	Deflection corresponding to different points of the slab								
	0	20	30	45	60	90	120	150	180
1	18.46	14.45	12.94	11.05	9.8	7.35	5.53	4.4	4.04
2	32.8	29.09	26.72	22.99	20.81	17.09	13.88	10.74	9.53
3	23.7	19.59	18.59	16.05	13.98	10.23	7.46	5.88	5.36
4	28.87	20.62	17.87	14.74	13.00	9.53	7.41	5.83	5.35
5	14.3	14.13	4.92	4.95	4.69	4.02	3.38	3.04	3.00
6	25.74	20.87	19.66	16.66	14.26	10.29	7.35	5.65	5.08
7	29.02	22.66	20.16	17.11	15.3	11.77	9.04	7.25	6.56
8	16.19	14.02	7.79	6.33	6.04	5.18	4.67	3.93	3.83

Figure 22: Field FWD detection.

Table 11: Judgment of soil foundation modulus, spring stiffness, and void degree.

Serial number	Exponential formula		Forecast classification		
	a	b	Elastic modulus of soil foundation	Spring stiffness	Void form and size
1	17.775	−0.010	100	0.01q	Full void of slab corner is 0.4 m
2	32.898	−0.007	100	0.01q	Full void of slab corner is 0.4 m
3	23.817	−0.009	80	0.01q	Half void at slab corner 0.4 m
4	26.921	−0.011	#N/A	0.005q	#N/A(not applicable)
5	13.954	−0.015	100	0.1q	Full void of slab corner is 0.4 m
6	25.805	−0.010	80	q	Full void of slab corner is 0.2 m
7	27.694	−0.009	80	q	Full void of slab corner is 0.2 m
8	14.973	−0.012	80	0.1q	Full void of slab corner is 0.2 m

The data in Table 10 are fitted with exponential curve formula.

Parameters a and b are obtained by fitting, and the corresponding contour maps, as the ones of Figures 19–21 are created to obtain the soil foundation elastic modulus, spring stiffness, void form, and size corresponding to different measured data, as shown in Table 11.

According to Figures 19–21, 7 groups of void problems can be identified, and 1 group cannot be identified, as it is beyond the scope of the model; the soil foundation elastic modulus is between 80 and 100 MPa for all groups, 6 groups are full void of slab corner, and 1 group is half void at slab corner. These are in agreement with the actual results, so the prediction is satisfactory.

8. Conclusions

A detailed analysis and design of the composite pavement cement concrete slab, evaluating accurately the spring stiffness, void size, and soil base elastic modulus at the bottom of cement concrete slab, could provide useful guidelines for its best maintenance and service performance. Therefore, the changing law of load transfer efficiency of cement concrete slab is revealed in this paper. Considering spring stiffness, void size, and soil base elastic modulus, the void evaluation method of composite pavement cement concrete slab is established by using back propagation neural network algorithm. The main conclusions are as follows:

(1) The spring simulation joint loading algorithm was compiled by Python, and the three-dimensional finite element model interpreting the different transfer efficiency was established. The influence of four factors (asphalt layer elastic modulus and thickness, cement concrete slab elastic modulus and thickness, modulus of foundation ground, and interlayer friction coefficient) on the load transfer efficiency of the joints under different values of spring stiffness was analyzed. The modulus of foundation ground had the greatest influence on the joint load transfer and the interlayer friction coefficient had the smallest.

(2) The calculation results of fixed spring stiffness, different void size, and degree show that the void reduces the load transfer efficiency of the joint, while the spring can effectively restrain the deformation of cement concrete slab under a certain void size and degree. If the spring exceeds the range, the elastic inhibition will decrease or fail.

(3) Based on BP neural network algorithm, a composite pavement void detection and evaluation method considering spring stiffness, void size, and soil elastic modulus is constructed. The evaluation method can adaptively discover the hidden information of void and joint stiffness to create the deflection basin. At the same time, the concise determination steps and void determination Atlas meeting the requirements of engineering application are given. In order to render the void evaluation method suitable for more complex engineering environment, more types of cement concrete slabs, such as reinforced concrete slabs, fiber reinforced concrete slabs, and prestressed concrete slabs, should be considered in future research.

Data Availability

The test data used to support the findings of this study have been deposited in the Hindawi Advance in Materials Science and Engineering repository. The test data are included within the article and can be made freely available.

Conflicts of Interest

The authors declare no conflicts of interest.

Acknowledgments

This research was funded by Construction of Science and Technology Projects by Ministry of Communications of China (2018-MS2-042), the Guangdong Province Transportation Science and Technology Project of China (2012-02-011), the Foshan City Transportation Science and Technology Project of China (2018AB003841), and 03 Special and 5G Projects in Jiangxi Province (20212ABC03A19).

References

[1] L. Liu, Z. Liu, J. Liu, and S. Li, "Fatigue performance of interlaminar anticracking material for rigid-flexible composite pavement," *Journal of Materials in Civil Engineering*, vol. 28, no. 10, Article ID 06016012, 2016.

[2] J. Huang, D. Huang, W. Li et al., "Fractal analysis on pore structure and hydration of magnesium oxysulfate cements by first principle, thermodynamic and microstructure-based methods," *Fractal and Fractional*, vol. 5, no. 4, p. 164, 2021.

[3] N. Fang, H. Li, Q. Li, X. Wang, S. Hu, and L. Xin, "Study on asphalt layer of composite pavement temperature shrinkage stress considering stress relaxation," *Materials and Structures*, vol. 54, no. 1, pp. 1–16, 2021.

[4] N. Kawamura, Y. Tsubokawa, and E. Kato, "Detection method of voids under concrete slab by using FWD," *Journal of Japan Society of Civil Engineers, Ser. E1 (Pavement Engineering)*, vol. 73, no. 1, pp. 1–11, 2017.

[5] X. Z. Xiao and Q. S. Li, "Study of method for identify void beneath cement concrete pavement slabs: a case study of meiguan expressway," *Journal of Highway and Transportation Research and Development*, vol. 33, no. 04, pp. 39–45+65, 2016.

[6] X. Q. Xiao, *Re1ationship between Voids beneath Slab and the Load Transfer Efficiency*, Southwest Jiaotong University, Sichuan, China, 2007.

[7] B. Vanden, "Effects of Slab Temperature Profiles on Use of Falling Weight Deflectometer Data to Monitor Joint Performance and Detect Voids," *Transportation Research Record Journal of the Transportation Research Board*, vol. 2005, pp. 75–85, 2007.

[8] M. Li, N. Anderson, L. Sneed, and E. Torgashov, "Condition assessment of concrete pavements using both ground

penetrating radar and stress-wave based techniques," *Journal of Applied Geophysics*, vol. 135, no. 1, pp. 297–308, 2016.

[9] A. Joshaghani, D. G. Zollinger, Concrete Pavements Curing Evaluation with Non-destructive Tests," *Construction and Building Materials*, vol. 154, 2017.

[10] W. W. L. Lai, R. K. W. Chang, and J. F. C. Sham, "A blind test of nondestructive underground void detection by ground penetrating radar (GPR)," *Journal of Applied Geophysics*, vol. 149, pp. 10–17, 2018.

[11] L. W. Miao, *The Analysis of Mechanics Response of Cement concrete Pavement with Void and Joint Load Transfer Coupling*, Southwest Jiaotong University, Sichuan, China, 2016.

[12] X. Y. Chen and L. H. Yin, "Method of PCC pavement void detection based on FEA," *Highways*, vol. 11, pp. 143–147, 2011.

[13] N. H. Zhang and M. Xiao, "Analysis of doweled joints under repetitive loading," *Journal of Southeast University*, vol. 2, pp. 91–97, 1998.

[14] K. Alland, J. Brigham, J. M. Vandenbossche, and J. Brigham, "Statistical model to detect voids for curled or warped concrete pavements," *Transportation Research Record: Journal of the Transportation Research Board*, vol. 2639, no. 1, pp. 28–38, 2017.

[15] J. A. Crovetti and M. I. Darter, "Void detection for jointed concrete pavements," *Transportation Research Record*, vol. 1041, pp. 59–68, 1985.

[16] S. J. Tong, Y. E. Cong, Q. Wang, and W. U. Lin-Jie, "Research on fatigue life prediction of cement pavement with void," *Journal of Guangxi University(Natural Science Edition)*, vol. 43, no. 01, pp. 304–313, 2018.

[17] N. Karballaeezadeh, F. Zaremotekhases, S. Shamshirband, Intelligent road inspection with advanced machine learning; hybrid prediction models for smart mobility and transportation maintenance systems," *Energies*, vol. 13, 2020.

[18] N. Fang, X. Wang, H. Ye, Y. Sun, Z. Su, and L. Yuan, "Study on fatigue characteristics and interlayer design method of waterproof cohesive bridge deck layer," *Applied Sciences*, vol. 9, no. 10, p. 2090, 2019.

[19] X. Wang, N. Fang, H. Ye, and J. Zhao, "Fatigue damage analysis of cement-stabilized base under construction loading," *Applied Sciences*, vol. 8, no. 11, pp. 2263–2283, 2018.

[20] Ministry of Communications of the People's Republic of China, *JTG D50 Specifications for Design of Highway Asphalt Pavement*, China Communications Press, Beijing, China, 2017.

[21] H. Ye, X. Wang, N. Fang, and Z. Su, "Low-temperature performance and evaluation index of gussasphalt for steel bridge decks," *Advances in Materials Science and Engineering*, vol. 201911 pages, 2019.

[22] L. Wang, X. Song, H. Yang, L. Wang, S. Tang, B. Wu, and W. Mao, Pore structural and fractal analysis of the effects of MgO reactivity and dosage on permeability and F–T resistance of concrete," *Fractal and Fractional*, vol. 113, no. 2, 2022.

[23] D. Y. Park, N. Buch, and K. Chatti, "Effective layer temperature prediction model and temperature correction via falling weight deflectometer deflections," *Transportation Research Record Journal of the Transportation Research Board*, vol. 1764, pp. 97–111, 2001.

[24] H. Li, N. Fang, X. Wang, C. Wu, and Y. Fang, "Evaluation of the coordination of structural layers in the design of asphalt pavement," *Applied Sciences*, vol. 10, no. 9, p. 3178, 2020.

[25] J. H. Song and P. F. Xin, "Geometric characteristics of asphalt pavement deflection basin under FWD load," *Journal of Chongqing Jianzhu University*, vol. 39, no. 11, pp. 92–98+108, 2020.

[26] J. Shi, *Matlab Program Design and Mathematical experiment and Modeling*, Beihang University Press, Beijing, China, 2019.

[27] Y. Deng, X. Luo, F. Gu, Y. Zhang, and R. L. Lytton, "3D simulation of deflection basin of pavements under high-speed moving loads," *Construction and Building Materials*, vol. 226, 2019.

[28] M. Pinzolas, A. Toledo, and J. L. Pedreño, "A neighborhood-based enhancement of the gauss-Newton bayesian regularization training method," *Neural Computation*, vol. 18, no. 8, pp. 1987–2003, 2006.